

Probing D_s^* -meson longitudinal twist-2 LCDA

Si-Hai Zhang,¹ Tao Zhong,^{1,2} Hai-Bing Fu,^{1,2,*} Ya-Xiong Wang,¹ and Wan-Bing Luo¹

¹Department of Physics, Guizhou Minzu University, Guiyang 550025, P.R.China

²Institute of High Energy Physics, Chinese Academy of Sciences, Beijing 100049, P.R.China

(Dated: March 11, 2025)

In this paper, we carry on an investigation of the semileptonic decays $B_s \rightarrow D_s^* \ell \bar{\nu}_\ell$. Firstly, we derive the moments of the D_s^* -meson longitudinal leading-twist light-cone distribution amplitude (LCDA) based on QCD sum rules within background field theory framework. Considering the contributions of the vacuum condensates up to dimension-six, its first ten non-zero ξ -moments at the initial scale $\mu_0 = 1$ GeV are $\langle \xi_{2;D_s^*}^{\parallel,1} \rangle|_{\mu_0} = -0.328_{-0.051}^{+0.041}$, $\langle \xi_{2;D_s^*}^{\parallel,2} \rangle|_{\mu_0} = +0.260_{-0.039}^{+0.045}$, $\langle \xi_{2;D_s^*}^{\parallel,3} \rangle|_{\mu_0} = -0.130_{-0.020}^{+0.016}$, $\langle \xi_{2;D_s^*}^{\parallel,4} \rangle|_{\mu_0} = +0.111_{-0.016}^{+0.018}$, $\langle \xi_{2;D_s^*}^{\parallel,5} \rangle|_{\mu_0} = -0.071_{-0.011}^{+0.009}$, $\langle \xi_{2;D_s^*}^{\parallel,6} \rangle|_{\mu_0} = +0.056_{-0.008}^{+0.009}$, $\langle \xi_{2;D_s^*}^{\parallel,7} \rangle|_{\mu_0} = -0.044_{-0.007}^{+0.006}$, $\langle \xi_{2;D_s^*}^{\parallel,8} \rangle|_{\mu_0} = +0.039_{-0.006}^{+0.007}$, $\langle \xi_{2;D_s^*}^{\parallel,9} \rangle|_{\mu_0} = -0.027_{-0.004}^{+0.003}$ and $\langle \xi_{2;D_s^*}^{\parallel,10} \rangle|_{\mu_0} = +0.028_{-0.004}^{+0.005}$, respectively. Meanwhile, we construct the D_s^* -meson longitudinal leading-twist LCDA by using the light-cone harmonic oscillator model. Then, using those moments, we fix the model parameters $\alpha_{2;D_s^*}$ and $B_1^{2;D_s^*}$ by the least square method and apply them to calculate $B_s \rightarrow D_s^*$ transition form factors $A_1(q^2)$, $A_2(q^2)$ and $V(q^2)$ that are derived by using the QCD light-cone sum rules. At the large recoil region, we obtain $A_1(0) = 0.632_{-0.135}^{+0.228}$, $A_2(0) = 0.706_{-0.092}^{+0.109}$ and $V(0) = 0.647_{-0.069}^{+0.076}$. Those form factors are then extrapolated to the allowed whole physical q^2 -region through the simplified series expansion. Finally, we obtain the branching fractions for the two decay channels $B_s \rightarrow D_s^* \ell \bar{\nu}_\ell$, *i.e.* $\mathcal{B}(B_s^0 \rightarrow D_s^{*+} e^- \bar{\nu}_e) = (5.45_{-1.57}^{+2.15}) \times 10^{-2}$, $\mathcal{B}(B_s^0 \rightarrow D_s^{*+} \mu^- \bar{\nu}_\mu) = (5.43_{-1.57}^{+2.14}) \times 10^{-2}$.

PACS numbers:

I. INTRODUCTION

B -meson semileptonic decay is one of the very important tools for studying the weak decay interaction. It have great phenomenological implications within the Standard Model (SM) of particle physics. The $B_s \rightarrow D_s^* \ell \bar{\nu}_\ell$ decay provides an opportunity for extracting CKM matrix elements and testing the SM [1–4]. Recently, the study of $B_s \rightarrow D_s^* \ell \bar{\nu}_\ell$ has attracted significant interest, driven by advancements in experimental capabilities and theoretical developments. Many experiments have provided more and more precise data of these decays, which allow the extraction of the CKM matrix element to an increasingly better accuracy. In addition, many theoretical groups have also generated great interest in exploring the decay channel.

In 2020, the LHCb Collaboration [5, 6] published an article on the experimental measurement of $B_s \rightarrow D_s^* \ell \bar{\nu}_\ell$ decay. They used the experimental data samples collected by the LHCb detector at the center-of-mass energies of 7 and 8 TeV and conducted systematic studies on the two decay channels $B_s^0 \rightarrow D_s^- \mu^+ \nu_\mu$ and $B_s^0 \rightarrow D_s^{*-} \mu^+ \nu_\mu$ using Caprini-Lellouch-Neubert (CLN) and Boyd-Grinstein-Lebed (BGL) parameterizations. Finally, the measured values of $|V_{cb}|$ obtained under the two parameterizations are $(41.4 \pm 0.6 \pm 0.9 \pm 1.2) \times 10^{-3}$ and $(42.3 \pm 0.8 \pm 0.9 \pm 1.2) \times 10^{-3}$, respectively. In reference [7], the lattice QCD and HPQCD Collaboration worked together to determine the model independent value of $V_{cb} = 39.03(56)_{\text{exp.}}(67)_{\text{latt.}} \times 10^{-3}$ using the $B \rightarrow D^* \ell \bar{\nu}_\ell$ data from Belle and the $B_s \rightarrow D_s^* \mu \bar{\nu}_\mu$ data from LHCb, as well as their

own transition form factors (TFFs). In addition, the TFFs and decay width behaviors for the $B_s \rightarrow D_s^* \ell \bar{\nu}_\ell$ process are also given in the article.

Theoretically, there are many theoretical methods for making reasonable theoretical predictions of $B_s \rightarrow D_s^* \ell \bar{\nu}_\ell$ decay, such as lattice QCD (LQCD) [8–12], covariant confined quark model (CCQM) [13], QCD sum rules (QCDSR) [14], relativistic quark model (RQM) [15], perturbative QCD (pQCD) [16, 17], light-front quark model (LFQM) [18], and bethe-salpeter method [19]. Then we provides a brief introduction to the above methods. In Ref. [9], the SM semileptonic vector and axial-vector form factors for $B_s \rightarrow D_s^*$ decay are calculated via the LQCD. The relevant calculation methods, the dependence on the heavy quark mass, decay rates and ratios are analysed. Meanwhile, the consistency with LHCb results and the tests on the impact of new physics couplings are also discussed. They give a reasonable reference to study the semileptonic decay of $B_s \rightarrow D_s^* \ell \bar{\nu}_\ell$. In Ref. [13], the author relies on the Standard Model framework based on the CCQM to carry out the calculation of TFFs within the entire dynamical category of squared momentum transfer for semileptonic decays. The obtained results, such as decay width ratios, show a degree of consistency with LHCb experiments and LQCD simulations, and the behaviors of differential decay distributions are compared. Meanwhile, other physical observations are also calculated. Through calculation, $R(D_s) = 0.271 \pm 0.069$, $R(D_s^*) = 0.240 \pm 0.038$ are obtained, and the ratio of decay widths of the D_s and D_s^* channels in the muon meson mode $\Gamma(B_s \rightarrow D_s \mu^+ \nu_\mu) / \Gamma(B_s \rightarrow D_s^* \mu^+ \nu_\mu) = 0.451 \pm 0.093$ is determined. In Ref. [14], the phenomenology of the b -flavored strange meson B_s^0 is studied through the QCDSR. Specifically, this includes the evaluation of the particle's mass and leptonic constant, as well as the study of the form factors of certain de-

*Electronic address: fuhb@gzmu.edu.cn

cays (such as $\bar{B}_s^0 \rightarrow D_s^+ \ell^- \bar{\nu}$, $\bar{B}_s^0 \rightarrow D_s^{*+} \ell^- \bar{\nu}$, $\bar{B}_s^0 \rightarrow K^{*+} \ell^- \bar{\nu}$); at the same time, the calculation of two-body non-leptonic \bar{B}_s^0 decays is carried out under the factorization approximation; finally, the evaluation result of the $SU(3)_F$ breaking effect in the \bar{B}_s^0 channel is compared with other estimates.

Also as a well-established theory that can be effectively applied to the exclusive decay process, the QCD light-cone sum rule (LCSR) [20, 21] incorporates both the hard and soft contribution in the computation of hadron transitions. In the LCSR method, the two-point correlation function of vacuum to meson is constructed for calculating heavy-to-light TFFs. In which, the matrix elements of nonlocal operators is carried out at light-cone region $x^2 \rightarrow 0$. The difference between this method and the traditional SVZ sum rule [22] is that the all non-perturbative dynamics are parameterized according to the light-cone distribution amplitudes (LCDAs) with progressively higher twists instead of quark and gluon condensates [23]. Currently, the LCSR has been widely applied to the study of B light-flavor meson decays [24–29]. In this work, we will adopt LCSR to calculate the $B_s \rightarrow D_s^*$ TFFs. Specifically, due to the presence of both longitudinal (\parallel) and transverse (\perp) polarization states in vector mesons, employing traditional currents to construct correlation functions poses a challenge involving fifteen LCDAs. Therefore, to simplify the calculation process, we will adopt chiral currents instead of traditional currents, allowing the contributions of twist-2 LCDA to dominate and eliminating contributions from other LCDAs. The specific procedure will be elaborated in the next section. Therefore, an accurate prediction of the twist-2 $\phi_{2,D_s^*}^{\parallel}(x, \mu)$ is of great importance. So far, the LCDA of many mesons depends on Gegenbauer moment, which can be calculated using additional sum rules. As a mature theoretical method, the background field theory (BFT) decomposes the quark field into a classical background field that describes non-perturbative effects and a quantum field that describes perturbative effects. This can provide a clean physical picture for separating the perturbative and non-perturbative properties of the QCD theory and provide a systematic way to derive the QCDSR for hadron phenomenology. Meanwhile, due to the ability to adopt different gauges for quantum fluctuations and the background field in BFT, the calculations can be greatly simplified. In our previous work, the longitudinal twist-2 LCDA of ρ -meson is successfully studied in BFT and constructed by light cone harmonic oscillator (LCHO) model [30]. Motivated by this, in this work, we will employ the BFT method to study the twist-2 LCDA of D_s^* -meson and attempt to integrate the phenomenological LCHO model to provide us with another perspective to understand the momentum distribution of quarks and gluons inside D_s^* -mesons.

The rest of this article are organized as follows. In Sec. II, we derive the summation rules for the ξ -moments of the D_s^* -meson longitudinal leading-twist $\phi_{2,D_s^*}^{\parallel}(x, \mu)$ LCDAs and the $B_s \rightarrow D_s^*$ TFFs $A_1(q^2)$, $A_2(q^2)$ and $V(q^2)$, and established the LCHO for the D_s^* -meson leading-twist LCDAs. In Sec. III, we provide relevant numerical results and make a detailed discussion. Section IV is reserved for summary.

II. THEORETICAL FRAMEWORK

The differential decay width of semileptonic decays $B_s \rightarrow D_s^* \ell \bar{\nu}_\ell$ can be written in terms of the helicity components basis [31–33]:

$$\frac{d\Gamma(B_s \rightarrow D_s^* \ell \bar{\nu}_\ell)}{dq^2} = \frac{G_F^2 |V_{cb}|^2 \lambda^{1/2} q^2}{192\pi^3 m_{B_s}^3} \left(1 - \frac{m_\ell^2}{q^2}\right) \mathcal{H}_{\text{total}}, \quad (1)$$

where the Fermi coupling constant $G_F = 1.1663787(6) \times 10^{-5} \text{ GeV}^{-2}$, $|V_{cb}|$ is the CKM matrix element, $\lambda \equiv \lambda(m_{B_s}^2, m_{D_s^*}^2, q^2) = m_{B_s}^4 + m_{D_s^*}^4 + q^4 - 2(m_{B_s}^2 m_{D_s^*}^2 + m_{B_s}^2 q^2 + m_{D_s^*}^2 q^2)$ is the phase-space factor, m_ℓ stands for the lepton mass ($\ell = e, \mu, \tau$), and $\mathcal{H}_{\text{total}}$ represents the overall helicity structure:

$$\mathcal{H}_{\text{total}} = (\mathcal{H}_U + \mathcal{H}_L) \left(1 + \frac{m_\ell^2}{2q^2}\right) + \frac{3m_\ell^2}{2q^2} \mathcal{H}_S. \quad (2)$$

The symbols \mathcal{H}_I ($I = U, L, S$) are the bilinear combinations of the helicity components of the hadronic tensor. Here, in this work the lepton mass m_ℓ is very small in case of $\ell = (e, \mu)$ when compared with the squared transition momentum q^2 , which can be safely neglected. Thus there will only leaves two helicity structures, *i.e.* \mathcal{H}_U and \mathcal{H}_L which have the following formulas

$$\mathcal{H}_U = |H_+|^2 + |H_-|^2, \quad \mathcal{H}_L = |H_0|^2. \quad (3)$$

The helicity amplitudes H_i with the index $i = (\pm, 0, t)$ are denoted as the function of invariant mass q^2 , which are formed from the $B_s \rightarrow D_s^*$ TFFs with different combinations:

$$\begin{aligned} H_\pm(q^2) &= (m_{B_s} + m_{D_s^*}) A_1(q^2) \mp \frac{\lambda^{1/2}}{m_{B_s} + m_{D_s^*}} V(q^2), \\ H_0(q^2) &= \frac{1}{2m_{D_s^*} \sqrt{q^2}} \left[(m_{B_s} + m_{D_s^*}) (m_{B_s}^2 - m_{D_s^*}^2 - q^2) \right. \\ &\quad \left. \times A_1(q^2) - \frac{\lambda}{m_{B_s} + m_{D_s^*}} A_2(q^2) \right], \end{aligned} \quad (4)$$

As we know, the three $B_s \rightarrow D_s^*$ TFFs $A_1(q^2)$, $A_2(q^2)$ and $V(q^2)$ are the important hadronic inputs for studying the relevant implications of semileptonic decays $B_s \rightarrow D_s^* \ell \bar{\nu}_\ell$. Therefore, to derive their analytic expressions within the LCSR approach, we construct the following chiral current correlation function (correlator):

$$\Pi_\mu(p, q) = i \int d^4x e^{iq \cdot x} \langle D_s^*(p) | T \{ J_\mu(x), J_{B_s}^\dagger(0) \} | 0 \rangle, \quad (5)$$

where $J_\mu(x) = \bar{c}(x) \gamma_\mu (1 + \gamma_5) b(x)$ and $J_{B_s}^\dagger(0) = \bar{b}(0) i (1 + \gamma_5) s(0)$ is the left-handed current. As the D_s^* -meson DAs are relatively complex structures, there are both chiral-even and chiral-odd DAs for D_s^* -meson, which has longitudinal and transverse polarization states. The adopted left-handed current can effectively high-light the contributions from the chiral-even DAs such as

$\phi_{2;D_s^*}^{\parallel}(x, \mu), \phi_{3;D_s^*}^{\perp}(x, \mu), \psi_{3;D_s^*}^{\perp}(x, \mu), \Phi_{3;D_s^*}^{\parallel}(x, \mu), \tilde{\Phi}_{3;D_s^*}^{\parallel}, \phi_{4;D_s^*}^{\parallel}(x, \mu)$, and $\psi_{4;D_s^*}^{\parallel}(x, \mu)$, while the chiral-odd DAs provide zero contributions. For the remaining chiral-even DAs, only the $\phi_{2;D_s^*}^{\parallel}, \phi_{3;D_s^*}^{\perp}(x, \mu)$, and $\psi_{3;D_s^*}^{\perp}(x, \mu)$ account for dominant contributions to the LCSR, while other chiral-even DAs offer negligible contributions. Moreover, the twist-3 DAs $\phi_{3;D_s^*}^{\perp}(x, \mu)$ and $\psi_{3;D_s^*}^{\perp}(x, \mu)$ can be linked with $\phi_{2;D_s^*}^{\parallel}(x, \mu)$ under the Wandzura-Wilczek (WW) approximation [34, 35]:

$$\begin{aligned}\phi_{3;D_s^*}^{\perp;WW}(x, \mu) &= \frac{1}{2} \left[\int_0^x dv \frac{\phi_{2;D_s^*}^{\parallel}(v, \mu)}{v} + \int_x^1 dv \frac{\phi_{2;D_s^*}^{\parallel}(v, \mu)}{v} \right], \\ \psi_{3;D_s^*}^{\perp;WW}(x, \mu) &= 2 \left[\bar{x} \int_0^x dv \frac{\phi_{2;D_s^*}^{\parallel}(v, \mu)}{v} + x \int_x^1 dv \frac{\phi_{2;D_s^*}^{\parallel}(v, \mu)}{v} \right].\end{aligned}\quad (6)$$

Therefore, the longitudinal leading-twist $\phi_{2;D_s^*}^{\parallel}(x, \mu)$ may provide a dominant contribution, either directly or indirectly.

The correlation function (5) is defined at both the time-like and the space-like q^2 -regions. In the time-like q^2 -region, long distance quark-gluon interactions are dominant. The correlator can insert a complete set of the B_s -meson states with the same J^P quantum numbers to acquire the hadron expression in physical region. Meanwhile, in space-like region, the correlator can be treated by the OPE in deep Euclidean region with the coefficients being pQCD calculable. After matching the two results by the dispersion relation, the final LCSR can be obtained by applying the Borel transformation, which is used to suppress the less known continuum contributions, and subsequently the resultant $B_s \rightarrow D_s^*$ TFFs under the LCSR approach read off:

$$\begin{aligned}A_1(q^2) &= \frac{2m_b^2 m_{D_s^*} f_{D_s^*}^{\parallel}}{f_{B_s} m_{B_s}^2 (m_{B_s} + m_{D_s^*}) e^{-m_{B_s}^2/M^2}} \left\{ \int_0^1 \frac{du}{u} e^{-s(u)/M^2} \right. \\ &\times \left[\Theta(c(u, s_0)) \phi_{3;D_s^*}^{\perp}(u) - \frac{m_{D_s^*}^2}{uM^2} \tilde{\Theta}(c(u, s_0)) C_{D_s^*}^{\parallel}(u) \right] \\ &- m_{D_s^*}^2 \int D\alpha \int dv e^{-s(X)/M^2} \frac{1}{X^2 M^2} \Theta(c(X, s_0)) \\ &\times \left[\Phi_{3;D_s^*}^{\parallel}(\alpha) + \tilde{\Phi}_{3;D_s^*}^{\parallel}(\alpha) \right] \Big\},\end{aligned}\quad (7)$$

$$\begin{aligned}A_2(q^2) &= \frac{m_b^2 m_{D_s^*} (m_{B_s} + m_{D_s^*}) f_{D_s^*}^{\parallel}}{f_{B_s} m_{B_s}^2 e^{-m_{B_s}^2/M^2}} \left\{ 2 \int_0^1 \frac{du}{u} e^{-s(u)/M^2} \left[\frac{1}{uM^2} \right. \right. \\ &\times \tilde{\Theta}(c(u, s_0)) A_{D_s^*}^{\parallel}(u) + \frac{m_{D_s^*}^2}{uM^4} \tilde{\tilde{\Theta}}(c(u, s_0)) C_{D_s^*}^{\parallel}(u) \\ &\left. \left. + \frac{m_b^2 m_{D_s^*}^2}{4u^4 M^6} \tilde{\tilde{\tilde{\Theta}}}(c(u, s_0)) B_{D_s^*}^{\parallel}(u) \right] + m_{D_s^*}^2 \int D\alpha \int dv \right.\end{aligned}$$

$$\times \frac{e^{-s(X)/M^2}}{X^3 M^4} \Theta(c(X, s_0)) [\Phi_{3;D_s^*}^{\perp}(\tilde{\alpha}) + \tilde{\Phi}_{3;D_s^*}^{\perp}(\tilde{\alpha})] \Big\},\quad (8)$$

$$\begin{aligned}V(q^2) &= \frac{m_b^2 m_{D_s^*} (m_{B_s} + m_{D_s^*}) f_{D_s^*}^{\parallel}}{2f_{B_s} m_{B_s}^2 e^{-m_{B_s}^2/M^2}} \int_0^1 du e^{-s(u)/M^2} \frac{1}{u^2 M^2} \\ &\times \tilde{\Theta}(c(u, s_0)) \psi_{3;D_s^*}^{\perp}(u).\end{aligned}\quad (9)$$

The three simplified D_s^* -meson LCDAs $A_{D_s^*}^{\parallel}(u), B_{D_s^*}^{\parallel}(u)$, and $C_{D_s^*}^{\parallel}(u)$ are represented as follows, respectively:

$$A_{D_s^*}^{\parallel}(u) = \int_0^u dv \left[\phi_{2;D_s^*}^{\parallel}(v) - \phi_{3;D_s^*}^{\perp}(v) \right],\quad (10)$$

$$B_{D_s^*}^{\parallel}(u) = \int_0^u dv \phi_{4;D_s^*}^{\parallel}(v),\quad (11)$$

$$\begin{aligned}C_{D_s^*}^{\parallel}(u) &= \int_0^u dv \int_0^v dw \left[\psi_{4;D_s^*}^{\parallel}(w) + \phi_{2;D_s^*}^{\parallel}(w) \right. \\ &\left. - 2\phi_{3;D_s^*}^{\perp}(v) \right].\end{aligned}\quad (12)$$

Furthermore, $s(\varrho) = [m_b^2 - \bar{\varrho}(q^2 - \varrho m_{D_s^*}^2)]/\varrho$ with $\bar{\varrho} = (1 - \varrho)$ and ϱ refers to u or $X = (a_1 + va_3)$. $f_{D_s^*}^{\parallel}$ is the D_s^* -meson decay constant. The usual step function $\Theta(c(\varrho, s_0))$, where $c(\varrho, s_0) = us_0 - m_b^2 + \bar{u}q^2 - u\bar{u}m_{D_s^*}^2$ is defined such that if $c(\varrho, s_0) < 0$, it is zero; otherwise, it is 1. The definitions of $\tilde{\Theta}(c(u, s_0))$ and $\tilde{\tilde{\Theta}}(c(u, s_0))$ are

$$\begin{aligned}\int_0^1 \frac{du}{u^2 M^2} e^{-s(u)/M^2} \tilde{\Theta}(c(u, s_0)) f(u) \\ = \int_{u_0}^1 \frac{du}{u^2 M^2} e^{-s(u)/M^2} f(u) + \delta(c(u_0, s_0)),\end{aligned}\quad (13)$$

$$\begin{aligned}\int_0^1 \frac{du}{2u^3 M^4} e^{-s(u)/M^2} \tilde{\tilde{\Theta}}(c(u, s_0)) f(u) \\ = \int_{u_0}^1 \frac{du}{2u^3 M^4} e^{-s(u)/M^2} f(u) + \Delta(c(u_0, s_0)),\end{aligned}\quad (14)$$

where $\delta(c(u, s_0)) = e^{-s_0/M^2} f(u_0)/C_0$ with $C_0 = m_b^2 + u_0^2 m_{D_s^*}^2 - q^2$ and

$$\Delta(c(u, s_0)) = e^{-s_0/M^2} \left[\frac{1}{2u_0 M^2} \frac{f(u_0)}{C_0} - \frac{u_0^2}{2C_0} \frac{d}{du} \left(\frac{f(u)}{uC} \right) \Big|_{u=u_0} \right].\quad (15)$$

At the stage, we shall focus on the longitudinal leading-twist DAs of D_s^* -meson. According to our previous works [36–38], which show the technique for constructing the LCHO model of vector mesons's wavefunction (WF) based on the Brodsky-Huang-Lepage (BHL) [39, 40], one can obtain

$$\Psi_{2;D_s^*}^{\parallel}(x, \mathbf{k}_{\perp}) = \sum_{\lambda_1 \lambda_2} \chi_{2;D_s^*}^{\lambda_1 \lambda_2}(x, \mathbf{k}_{\perp}) \Psi_{2;D_s^*}^R(x, \mathbf{k}_{\perp})$$

$$= \frac{\tilde{m}}{\sqrt{\mathbf{k}_\perp^2 + \tilde{m}^2}} A_{2;D_s^*} \varphi_{2;D_s^*}(x) \times \exp \left[-\frac{1}{\beta_{2;D_s^*}^2} \left(\frac{\mathbf{k}_\perp^2 + \hat{m}_c^2}{1-x} + \frac{\mathbf{k}_\perp^2 + \hat{m}_s^2}{x} \right) \right], \quad (16)$$

where equivalent mass $\tilde{m} = \hat{m}_c x + \hat{m}_s (1-x)$ with \hat{m}_c and \hat{m}_s refer to the constituent quark masses and $\lambda_{1(2)}$ are the helicities of two constituent quarks. $A_{2;D_s^*}$ is the normalization constant, $\beta_{2;D_s^*}$ governs the transverse distribution, and $\varphi_{2;D_s^*}(x) = 1 + B_1^{2;D_s^*} C_1^{3/2}(2x-1)$ governs the longitudinal distribution. By considering the relation between the leading-twist DA and its WF,

$$\phi_{2;D_s^*}^\parallel(x, \mu_0^2) = \frac{2\sqrt{6}}{f_{D_s^*}^\parallel} \int_{|\mathbf{k}_\perp|^2 \leq \mu_0^2} \frac{d^2 \mathbf{k}_\perp}{16\pi^3} \Psi_{2;D_s^*}^\parallel(x, \mathbf{k}_\perp), \quad (17)$$

one can derive the leading-twist DA $\phi_{2;D_s^*}^\parallel(x, \mu_0^2)$ after integrating the transverse momentum \mathbf{k}_\perp :

$$\begin{aligned} \phi_{2;D_s^*}^\parallel(x, \mu_0^2) &= \frac{\sqrt{6} A_{D_s^*} \beta_{2;D_s^*}^2}{\pi^2 f_{D_s^*}^\parallel} x(1-x) \varphi_{2;D_s^*}^\parallel(x, \mu) \\ &\times \exp \left[-\frac{x \hat{m}_c^2 + (1-x) \hat{m}_s^2}{8\beta_{2;D_s^*}^2 x(1-x)} \right] \\ &\times \left\{ 1 - \exp \left[-\frac{\mu_0^2}{8\beta_{2;D_s^*}^2 x(1-x)} \right] \right\}, \quad (18) \end{aligned}$$

where $\mu_0 \sim \Lambda_{\text{QCD}}$ represents the factorization scale. Additionally, the model parameters $A_{2;D_s^*}$, $\beta_{2;D_s^*}$, and $B_1^{2;D_s^*}$ can be appropriately determined by relative constraints, such as the $\phi_{2;D_s^*}^\parallel(x, \mu_0^2)$ normalization condition, the Fock-state expansion of the D_s^* -meson, and the Gegenbauer moments of $\phi_{2;D_s^*}^\parallel(x, \mu_0^2)$ [36–38].

On the other hand, considering the definitions of the leading-twist DA $\phi_{2;D_s^*}^\parallel(x, \mu)$,

$$\begin{aligned} \langle 0 | \bar{c}(z) \not{z} \gamma_5 s(-z) | D_s^*(q) \rangle &= i(z \cdot q) f_{D_s^*}^\parallel \\ &\times \int_0^1 dx e^{i(2x-1)(z \cdot q)} \phi_{2;D_s^*}^\parallel(x, \mu), \quad (19) \end{aligned}$$

and

$$\langle \xi_{2;D_s^*}^{\parallel;n} \rangle |_\mu = \int_0^1 dx (2x-1)^n \phi_{2;D_s^*}^\parallel(x, \mu), \quad (20)$$

$$\langle \xi_{2;D_s^*}^{\parallel;0} \rangle |_\mu = \int_0^1 dx \phi_{2;D_s^*}^\parallel(x, \mu) = 1, \quad (21)$$

one can consider the following two-point correction function to derive the n th-order ξ -moments of D_s^* -meson,

$$\Pi_{2;D_s^*}^{(n,0)}(z, q) = i \int d^4 x i q \cdot x \langle 0 | T \{ J_n(x) J_0^\dagger(0) \} | 0 \rangle$$

$$= (z \cdot q)^{n+2} I_{2;D_s^*}^{(n,0)}(q^2). \quad (22)$$

The currents $J_n(x) = \bar{c}(x) \not{z} \gamma_5 (i z \cdot \overleftrightarrow{D})^n s(x)$ and $J_0^\dagger(0) = \bar{s}(0) \not{z} \gamma_5 c(0)$ can be derived from Eq. (19) by expanding the its l.h.s. around $z \rightsquigarrow 0$ and expanding the exponential on the r.h.s. of Eq. (19) into a power series. Subsequently, according to the method of BFTSR [41], one can get the analytical expression of the D_s^* -meson longitudinal leading-twist DA moments $\langle \xi_{2;D_s^*}^{\parallel;n} \rangle |_\mu$:

$$\begin{aligned} \langle \xi_{2;D_s^*}^{\parallel;n} \rangle |_\mu &= \frac{M^2 e^{m_{D_s^*}/M^2}}{f_{D_s^*}^{\parallel 2}} \left\{ \frac{1}{\pi M^2} \int_{t_{\min}}^{s_0^{D_s^*}} ds e^{-s/M^2} \text{Im } I_{\text{pert}}(s) \right. \\ &+ \hat{L}_M I_{\langle \bar{q}q \rangle}(-q^2) + \hat{L}_M I_{\langle G^2 \rangle}(-q^2) \\ &+ \hat{L}_M I_{\langle \bar{q}Gq \rangle}(-q^2) + \hat{L}_M I_{\langle \bar{q}q \rangle^2}(-q^2) \\ &\left. + \hat{L}_M I_{\langle G^3 \rangle}(-q^2) \right\}, \quad (23) \end{aligned}$$

The perturbative and each condensates terms with Borel transformation have the following forms

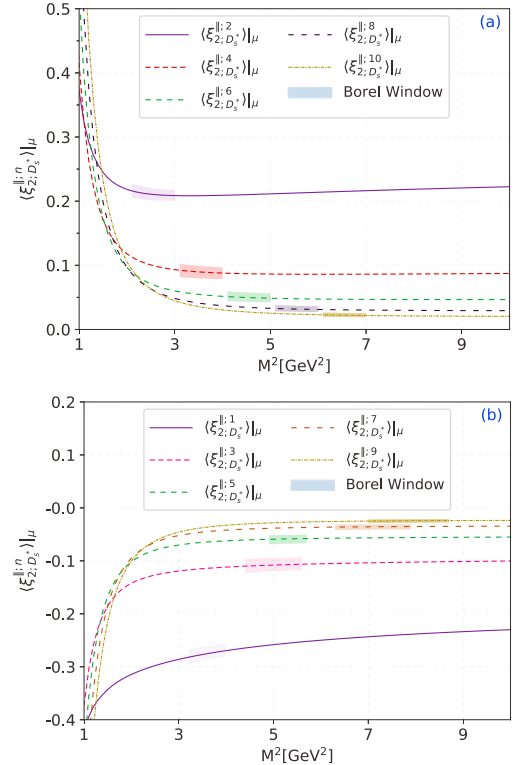


FIG. 1: The D_s^* -meson twist-2 LCDA moments $\langle \xi_{2;D_s^*}^{\parallel;n} \rangle |_\mu$ with $(n = 1, \dots, 10)$ versus the Borel parameter M^2 . Here, we only present the central values to show the curves of different moments clearly.

$$\text{Im}I_{\text{pert}}(s) = \frac{3}{8\pi(n+1)(n+3)} \left\{ \left[2(n+1) \frac{m_c^2}{s} \left(1 - \frac{m_c^2}{s} \right) + 1 \right] \left(1 - \frac{2m_c^2}{s} \right)^{n+1} + (-1)^n \right\}, \quad (24)$$

$$\hat{L}_M I_{\langle \bar{s}s \rangle}(-q^2) = (-1)^n \exp\left(-\frac{m_c^2}{M^2}\right) \frac{m_s \langle \bar{s}s \rangle}{M^4}, \quad (25)$$

$$\hat{L}_M I_{\langle G^2 \rangle}(-q^2) = \frac{\langle \alpha_s G^2 \rangle}{M^4} \frac{1}{12\pi} \left[2n(n-1) \mathcal{H}(n-2, 1, 1) + \mathcal{H}(n, 0, 0) - \frac{m_c^2}{M^2} \mathcal{H}(n, 1, -2) \right], \quad (26)$$

$$\hat{L}_M I_{\langle \bar{s}G_s \rangle}(-q^2) = (-1)^n \exp\left(-\frac{m_c^2}{M^2}\right) \frac{m_s \langle g_s \bar{s} \sigma T G_s \rangle}{M^6} \left(-\frac{8n+1}{18} - \frac{2m_c^2}{9M^2} \right), \quad (27)$$

$$\hat{L}_M I_{\langle \bar{s}s \rangle^2}(-q^2) = (-1)^n \exp\left(-\frac{m_c^2}{M^2}\right) \frac{\langle g_s \bar{s}s \rangle^2}{M^6} \frac{2(2n+1)}{81}, \quad (28)$$

$$\begin{aligned} \hat{L}_M I_{\langle G^3 \rangle}(-q^2) &= \frac{\langle g_s^3 f G^3 \rangle}{\pi^2 M^6} \left\{ \exp\left(-\frac{m_c^2}{M^2}\right) \left\{ -\frac{17}{96} \mathcal{F}_1(n, 5, 3, 2, \infty) + \frac{n}{144} \mathcal{F}_2(n-1, 5, 3, 1, \infty) - \frac{1}{96} \mathcal{F}_2(n, 4, 3, 1, \infty) \right. \right. \\ &+ \frac{1}{144} \mathcal{F}_2(n, 3, 3, 1, \infty) - \frac{17}{96} \mathcal{G}_1(n, 5) - \frac{17}{32} \mathcal{G}_2(n, 5) \left(1 - \frac{1}{3} \frac{m_c^2}{M^2} \right) + \frac{n}{144} \mathcal{G}_2(n-1, 5) - \frac{n}{96} \mathcal{G}_3(n, 4) + \frac{n}{144} \mathcal{G}_3(n, 3) \\ &+ \frac{1}{288} \left[204\delta^{n0} + 204\theta(n-1)(-1)^n + (-1)^n \left(100n - 154 + 51 \frac{m_c^2}{M^2} \right) \right] \left[\ln \frac{M^2}{\mu^2} + \psi(3) \right] + \frac{(-1)^n}{288} \left(17 \frac{m_c^2}{M^2} - 4n \right) \left. \right\} \\ &+ \left\{ \frac{1}{288} \left[-4(n+1)n(n-1) \mathcal{H}(n-2, 1, 1) + 4(n+1) \mathcal{H}(n, 0, 0) - 2n \mathcal{H}(n-1, 1, -1) - 3 \mathcal{H}(n, 0, -1) - 51 \mathcal{H}(n, 1, -2) \right] \right. \\ &+ \frac{1}{288} \frac{m_c^2}{M^2} \left[-4n(n-1) \mathcal{H}(n-2, 1, 0) 2 \mathcal{H}(n, 0, -2) + 4 \mathcal{H}(n, 0, -1) - 2 \mathcal{H}(n-1, 1, -2) - 3 \mathcal{H}(n, 1, -3) \right] + \frac{1}{240} \frac{m_c^4}{M^4} \\ &\left. \times \mathcal{H}(n, 1, -4) \right\}. \end{aligned} \quad (29)$$

In which, the definition about the hypergeometric function $\mathcal{F}_{1,2}(n, a, b, l_{\min}, l_{\max})$, $\mathcal{G}_{1,2,3}(n, a)$, $\mathcal{H}(n, a, b)$ and the traditional Borel transformation formulas $\hat{L}_M \frac{1}{(-q^2+m_c^2)^k} \ln \frac{-q^2+m_c^2}{\mu^2}$, $\hat{L}_M (-q^2+m_c^2)^k \ln \frac{-q^2+m_c^2}{\mu^2}$, $\hat{L}_M \frac{(-q^2)^l}{(-q^2+m_c^2)^{l+\tau}}$ can be found in our previous work [42–44]. Here, we have a notation that these functions have similar expressions in our previous work [44] with the difference about the light-quark and strange quark.

III. NUMERICAL ANALYSIS

For the subsequent numerical calculations, we adopt the following parameters: the mass of $m_{D_s^*}$ -meson is $m_{D_s^*} = 2.1122 \pm 0.0004$ GeV, c -quark current quark mass is $\bar{m}_c(\bar{m}_c) = 1.28 \pm 0.03$ GeV, the mass of s -quark is $\bar{m}_s(2 \text{ GeV}) = 0.0934^{+0.0086}_{-0.0034}$ GeV, and the decay constant of $m_{D_s^*}$ -meson is $f_{D_s^*} = f_{D_s^*}^{\parallel} = 0.279 \pm 0.019$ GeV [45]. Sometimes, when we need to evolve parameters to any other scale, we have to employ renormalization group equations (RGEs), and among them, certain inputs correspond to specific RGEs [46, 47].

$$\bar{m}_c(\mu) = \bar{m}_c(\bar{m}_c) \left[\frac{\alpha_s(\mu)}{\alpha_s(\bar{m}_c)} \right]^{\frac{12}{25}},$$

$$\bar{m}_s(\mu) = \bar{m}_s(2 \text{ GeV}) \left[\frac{\alpha_s(\mu)}{\alpha_s(2 \text{ GeV})} \right]^{\frac{12}{27}}. \quad (30)$$

Following by the usual convention, we set the scale near the Borel parameter, *i.e.*, $\mu = M$. For the continuous threshold $s_0^{D_s^*}$, we require a reasonable Borel window in Eq. (23) to normalize $\langle \xi_{2,D_s^*}^{\parallel;0} \rangle_{\mu_0} = 1$, such that the value of the continuum threshold is $s_0^{D_s^*} \simeq 6.8$ GeV².

After obtaining these input parameters, we can calculate the value of the ξ -moment by substituting them into the sum rule (23). In this article, we calculated the values of the first ten orders of the ξ -moments. In order to get a stable and appropriate Borel windows for the LCDA moments, we can use the usual criterion that the contributions from continuum states. That is we take the continuum contributions do not exceed 10%, 20%, 25%, 35%, 40% for the odd-order of $n = (1, 3, 5, 7, 9)$, respectively. Then we can get the upper limits of the corresponding Borel windows. For the lower limits Borel window we consider the contribution from dimension-six condensates are lower than 5%. The same conditions are also used in the even-order moments. Finally, we present the D_s^* -meson longitudinal leading-twist LCDA moments with $n = (2, 4, 6, 8, 10)$ and $n = (1, 3, 5, 7, 9)$ versus the Borel parameter M^2 in Fig. 1(a) and Fig. 1(b), separately. In which, the shaded bands are stand for the Borel windows. Then numerically

TABLE I: The first tenth-order ξ -moments of D_s^* -meson longitudinal twist-2 distribution amplitude $\phi_{2;D_s^*}^{\parallel}(x, \mu)$ at the scale $\mu_0 = 1.0$ GeV and $\mu_k = 3.0$ GeV.

	$\mu_0 = 1.0\text{GeV}$	$\mu_k = 3.0\text{ GeV}$
$\langle \xi_{2;D_s^*}^{\parallel:1} \rangle \mu$	$-0.328^{+0.041}_{-0.051}$	$-0.258^{+0.033}_{-0.039}$
$\langle \xi_{2;D_s^*}^{\parallel:2} \rangle \mu$	$+0.260^{+0.045}_{-0.039}$	$+0.179^{+0.031}_{-0.026}$
$\langle \xi_{2;D_s^*}^{\parallel:3} \rangle \mu$	$-0.130^{+0.016}_{-0.020}$	$-0.104^{+0.013}_{-0.016}$
$\langle \xi_{2;D_s^*}^{\parallel:4} \rangle \mu$	$+0.111^{+0.018}_{-0.016}$	$+0.083^{+0.014}_{-0.012}$
$\langle \xi_{2;D_s^*}^{\parallel:5} \rangle \mu$	$-0.071^{+0.009}_{-0.011}$	$-0.057^{+0.007}_{-0.009}$
$\langle \xi_{2;D_s^*}^{\parallel:6} \rangle \mu$	$+0.056^{+0.009}_{-0.008}$	$+0.045^{+0.008}_{-0.006}$
$\langle \xi_{2;D_s^*}^{\parallel:7} \rangle \mu$	$-0.044^{+0.006}_{-0.007}$	$-0.035^{+0.005}_{-0.006}$
$\langle \xi_{2;D_s^*}^{\parallel:8} \rangle \mu$	$+0.039^{+0.007}_{-0.006}$	$+0.031^{+0.005}_{-0.004}$
$\langle \xi_{2;D_s^*}^{\parallel:9} \rangle \mu$	$-0.027^{+0.003}_{-0.004}$	$-0.023^{+0.003}_{-0.004}$
$\langle \xi_{2;D_s^*}^{\parallel:10} \rangle \mu$	$+0.028^{+0.005}_{-0.004}$	$+0.022^{+0.004}_{-0.003}$

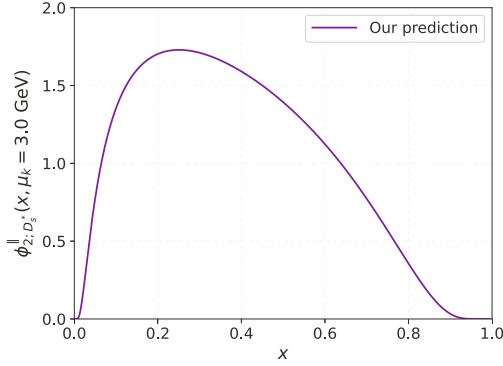


FIG. 2: The D_s^* -meson longitudinal leading-twist DA curves of our prediction at typical process scale $\mu_k = 3.0$ GeV.

cal results for the first ten order moments of D_s^* -meson twist-2 LCDAs at initial scale $\mu_0 = 1.0$ GeV and typical process scale $\mu_k = 3.0$ GeV are given in Table I.

Then, using the least squares method to fit the values of the ξ -moments in Table I with the LCHO model shown in Eq. (18), the behavior of the D_s^* -meson longitudinal twist-2 LCDA $\phi_{2;D_s^*}^{\parallel}(x, \mu)$ can be determined. Through the fitting method detailed in Refs. [48, 49], we determined the model parameters and corresponding goodness of fit. That is, by the magnitude of the probability $P_{\chi^2_{\min}} = \int_{\chi^2_{\min}}^{\infty} f(y; n_d) dy$ with the probability density function of $\chi^2(\theta)$, $f(y; n_d) = \frac{1}{\Gamma(n_d/2)2^{n_d/2}} y^{n_d/2-1} e^{-y/2}$, one can intuitively judge the goodness of fit. Here, n_d represents the number of degrees of freedom. The optimal values of model parameters $\alpha_{2;D_s^*}$, $B_1^{2;D_s^*}$, and $\beta_{2;D_s^*}$ at scale $\mu_k = 3.0$ GeV and their goodness of fit are shown as follows

$$A_{2;D_s^*}(\mu_k) = 9.421 \text{ GeV}^{-1};$$

TABLE II: The $B_s \rightarrow D_s^*$ TFFs at large recoil region, *i.e.* $A_1(0)$, $A_2(0)$ and $V(0)$ with uncertainties. Meanwhile, the comparison from theoretical groups are also given.

	$V(0)$	$A_1(0)$	$A_2(0)$
This work	$0.647^{+0.076}_{-0.069}$	$0.632^{+0.228}_{-0.135}$	$0.706^{+0.109}_{-0.092}$
CCQM [13]	0.743 ± 0.030	0.681 ± 0.065	0.630 ± 0.025
SR [14]	0.63 ± 0.05	0.62 ± 0.10	0.75 ± 0.07
RQM [15]	0.95 ± 0.02	0.70 ± 0.01	0.75 ± 0.02
PQCD [17]	0.64 ± 0.12	0.50 ± 0.09	0.53 ± 0.11
LFQM [18]	$0.74^{+0.05}_{-0.05}$	$0.61^{+0.04}_{-0.04}$	$0.59^{+0.04}_{-0.04}$

$$\begin{aligned}
\alpha_{2;D_s^*}(\mu_k) &= -0.860; \\
B_1^{2;D_s^*}(\mu_k) &= 0.025; \\
\beta_{2;D_s^*}(\mu_k) &= 0.774 \text{ GeV}; \\
\chi_{\min}^2(\mu_k) &= 2.463; \\
P_{\chi_{\min}^2}(\mu_k) &= 92.98\%.
\end{aligned} \tag{31}$$

Then, the D_s^* -meson longitudinal leading-twist LCDA can be determined. In order to display the behavior of $\phi_{2;D_s^*}^{\parallel}(x, \mu)$ clearly and visually, we plot its curve in Fig. 2.

Based on the resultant D_s^* -meson longitudinal leading-twist DA, we can then calculate the $B_s \rightarrow D_s^*$ TFFs $A_1(q^2)$, $A_2(q^2)$, $V(q^2)$. The basic input parameters are mentioned at the beginning of this section. Therefore, the main task is to determine the continuum threshold parameter s_0 and the Borel window M^2 . Based on the basic idea and process of LCSR, we have adopted the following three guidelines.

- The continuum contributions are less than 30% of the total results;
- The contributions from higher-twist DAs are less than 5%;
- Within the Borel window, the changes of TFFs does not exceed 10% ;
- The continuum threshold $s_0^{D_s^*}$ should be closer to the squared mass of the first excited state D_s^* -meson.

Based on the above criteria, we determined the values of the continuum threshold $s_0^{D_s^*}$ and the Borel window M^2 . According to the standard LCSR process, we calculated the final results of the TFFs and presented them in Table II. For comparison, we also give the results predicted by other theoretical groups CCQM [13], QCDSR [14], RQM [15], PQCD [17], LFQM [18]. By comparison, we can see that our predicted results are in good agreement with those predicted by these theoretical groups within the error range.

In order to access the information of $B_s \rightarrow D_s^* \ell \bar{\nu}_\ell$ TFFs in the whole kinematic region, we need to extrapolate the LCSR predictions obtained above toward large momentum transfer

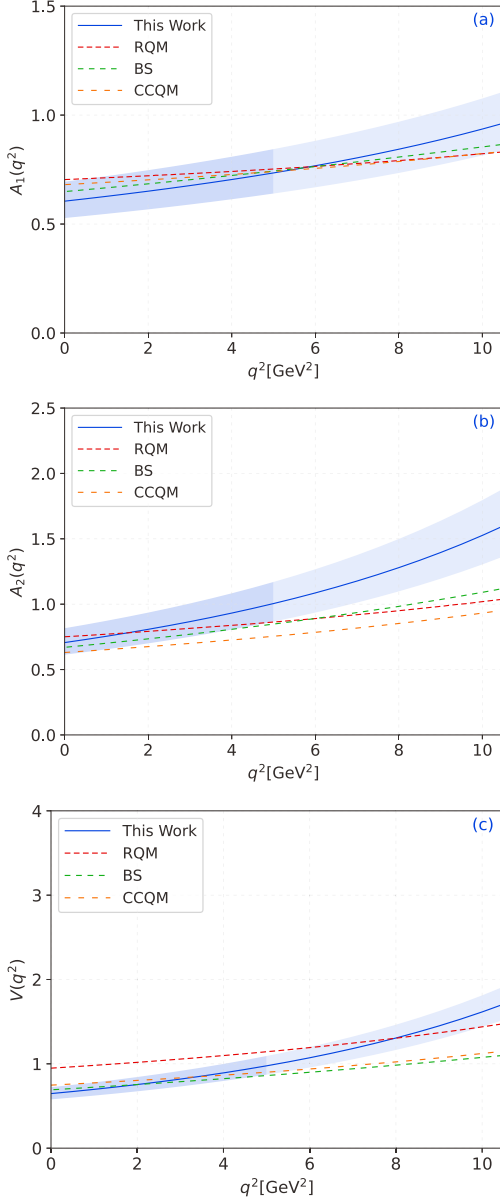


FIG. 3: The extrapolated TFFs $A_1(q^2)$, $A_2(q^2)$, $V(q^2)$ versus q^2 . The solid blue line is the central value, and the shaded band is the corresponding uncertainty. As a comparison, the predictions under the RQM [15] approach, the BS [19] approach, and the CCQM [52] approach are also presented

with a certain parametrization for the TFFs. The physically allowable ranges for the TFFs are $0 \leq q^2 \leq q_{\max}^2 = (m_{B_s} - m_{D_s^*})^2 \sim 10.6 \text{ GeV}^2$. Theoretically, the LCSR approach for $B_s \rightarrow D_s^* \ell \bar{\nu}_\ell$ TFFs is in low and intermediate q^2 -regions, *i.e.* $0 \leq q^2 \leq 5 \text{ GeV}^2$ of D_s^* -meson. One can extrapolate it to whole q^2 -regions via a rapidly $z(q^2, t)$ converging the simplified series expansion (SSE), *i.e.* the TFFs are expanded

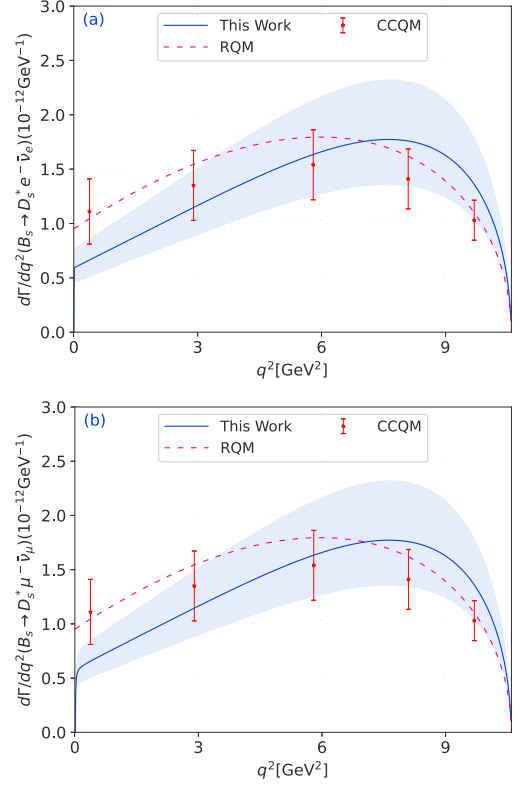


FIG. 4: Differential decay widths for $B_s \rightarrow D_s^* \ell \bar{\nu}_\ell$ in whole q^2 -region, where the solid line is the central value and the shaded band shows its uncertainty. As a contrast, this paper also introduces the use of different theoretical methods, such as CCQM [13], RQM [15].

as [50, 51]:

$$f_+(q^2) = \frac{1}{1 - q^2/m_{B_s^2}} \sum_{k=0,1,2} \beta_k z^k(q^2, t_0) \quad (32)$$

where β_k are real coefficients and $z(q^2, t)$ is the function,

$$z^k(q^2, t_0) = \frac{\sqrt{t_+ - q^2} - \sqrt{t_+ - t_0}}{\sqrt{t_+ - q^2} + \sqrt{t_+ - t_0}}, \quad (33)$$

with $t_{\pm} = (m_{B_s} \pm m_{D_s^*})^2$ and the auxiliary parameter $t_0 = t_{\pm}(1 - \sqrt{1 - t_-/t_+})$. The SSE method possesses superior merit, which keeps the analytic structure correct in the complex plane and ensures the appropriate scaling, $f_+(q^2) \sim 1/q^2$ at large q^2 . And the quality of fit Δ is devoted to take stock of the resultant of extrapolation, which is defined as

$$\Delta = \frac{\sum_t |F_i(t) - F_i^{\text{fit}}(t)|}{\sum_t |F_i(t)|} \times 100. \quad (34)$$

After making an extrapolation for the TFFs $A_1(q^2)$, $A_2(q^2)$, $V(q^2)$ to the physical q^2 -region, the behaviors of the $B_s \rightarrow D_s^* \ell \bar{\nu}_\ell$ TFFs in the whole physical region can be obtained. These behaviors have been given in Fig. 3. For comparison, we also present the results predicted by other theoretical groups for the TFFs, which are illustrated in detail in Fig. 3 below.

TABLE III: The branching fractions (in unit: %) for the decays $B_s^0 \rightarrow D_s^{*+} \ell \bar{\nu}_\ell$ with $\ell = (e, \mu)$ in this work. Meanwhile, the theoretical results are given as a comparison.

Decay Channel	$B_s^0 \rightarrow D_s^{*+} e^- \bar{\nu}_e$	$B_s^0 \rightarrow D_s^{*+} \mu^- \bar{\nu}_\mu$
This Work	$5.45^{+2.15}_{-1.57}$	$5.43^{+2.14}_{-1.57}$
PDG [5]	-	5.2 ± 0.5
CCQM [13]	6.42 ± 0.67	6.39 ± 0.67
RQM [15]	5.3 ± 0.5	-
LFQM [18]	-	5.2 ± 0.6
PQCD [17]	$4.42^{+1.27}_{-1.00}$	-

- In Fig. 3, the lighter band represents the LCSR results of our prediction, while the darker band represents the SSE predictions ;
- In the figure, the solid blue line represents this work. The red dotted line, the green dotted line, and the yellow dotted line represent the results predicted by RQM [15], CCQM [52], and Bethe-Salpeter method (BS) [19] respectively;
- In order to see the behavior of TFFs $A_1(q^2)$, $A_2(q^2)$, $V(q^2)$ more directly, as a comparison, we also show the predictions of theoretical groups such as RQM, CCQM, BS. In comparison, our results are found to be consistent within the appropriate margin of error.

The differential branching ratio is a very important physical observable measurement of the semileptonic decay process, and its study helps us to understand the internal structure of particles and their interactions with other particles. Therefore, it is very important to calculate $B_s \rightarrow D_s^* \ell \bar{\nu}_\ell$ semileptonic decay and its branching ratio. Here we use $|V_{cb}| = 0.041$ to calculate [5], and using the branching ratio formula, we can obtain the numerical result of the branching ratio. In addition, we also present the attenuation width diagram, as shown in Fig. 4. For comparison, we also show the predictions of other theoretical groups, including CCQM [13] and RQM [15]. By comparison, we can see that our results agree well with both experimental and theoretical predictions within a suitable error range.

In Table III, we comprehensively present the numerical results for the branching ratios of various decay channels associated with the semileptonic decay of $B_s \rightarrow D_s^* \ell \bar{\nu}_\ell$. Alongside our findings, we also showcase the numerical predictions offered by other leading theoretical groups, namely CCQM [13], RQM [15], LFQM [18], PQCD [17], and PDG [5]. Upon conducting a meticulous comparison among these results, we

notice that there exists a certain degree of deviation between our outcomes and those reported by the other groups. This discrepancy can likely be attributed to errors in the input parameters utilized in the respective calculations. Nevertheless, it is important to emphasize that, within a reasonable and acceptable range of error, our results are deemed to be valid and reliable.

IV. SUMMARY

This article studies the semileptonic decay process of $B_s \rightarrow D_s^* \ell \bar{\nu}_\ell$ within the framework of QCDSR. First, we present the expressions for the D_s^* -meson longitudinal twist LCDA moments $\langle \xi_{2;D_s^*}^{\parallel,n} \rangle |_\mu$, and list the values of the first ten ξ -moments at $\mu_0 = 1.0$ GeV and $\mu_k = 3.0$ GeV in Table I. Subsequently, we employed the least squares method to fit the values of the tenth-order ξ -moments at $\mu_k = 3.0$ GeV in order to determine the corresponding model parameters. Based on the BHL method, we constructed a new model of $\phi_{2;D_s^*}^{\parallel}(x, \mu)$, whose behavior is constrained by normalization conditions, the probability of finding the leading Fock-state in the D_s^* -meson Fock-state expansion, and known Gegenbauer moments. Research shows that it is necessary to find a more accurate form of meson DA. In the study of various processes, the error caused by using meson DA as an input parameter should be considered. In order to present the behavior of the LCDA $\phi_{2;D_s^*}^{\parallel}(x, \mu)$ in a clear and intuitive manner, we have depicted its curve in Fig. 2.

Then, we calculated $B_s \rightarrow D_s^* \ell \bar{\nu}_\ell$ TFFs $A_1(q^2)$, $A_2(q^2)$, $V(q^2)$ by using the LCSR method. We present the numerical results of the TFFs in the maximum buffer region in Table II. After extrapolating the LCSR results of $B_s \rightarrow D_s^*$ TFFs to the entire q^2 -region, the differential decay width and branching ratio of the semileptonic decay $B_s \rightarrow D_s^* \ell \bar{\nu}_\ell$ are obtained, as shown in Table III and Fig. 4. It was compared with other predictions and found to be consistent with experimental data and other methods within the error range.

V. ACKNOWLEDGMENTS

Tao Zhong and Hai-Bing Fu would like to thank the Institute of High Energy Physics of Chinese Academy of Sciences for their warm and kind hospitality. This work was supported in part by the National Natural Science Foundation of China under Grant No.12265009, No.12265010, the Project of Guizhou Provincial Department of Science and Technology under Grant No.ZK[2025]MS219, No.ZK[2023]024.

[1] J. P. Lees *et al.* [BABAR Collaboration], *Evidence for an excess of $\bar{B} \rightarrow D^{(*)} \tau^- \bar{\nu}_\tau$ decays*, *Phys. Rev. Lett.* **109**, 101802 (2012)

[arXiv:1205.5442]
[2] M. Huschle *et al.* [BELLE Collaboration], *Measurement of the*

- branching ratio of $\bar{B} \rightarrow D^{(*)} \tau^- \bar{\nu}_\tau$ relative to $\bar{B} \rightarrow D^{(*)} \ell^- \bar{\nu}_\ell$ decays with hadronic tagging at Belle, *Phys. Rev. D* **92**, 072014 (2015) [arXiv:1507.03233]
- [3] G. Caria *et al.* [BELLE Collaboration], *Measurement of $\mathcal{R}(D)$ and $\mathcal{R}(D^*)$ with a semileptonic tagging method*, *Phys. Rev. Lett.* **124**, 161803 (2020) [arXiv:1910.05864]
- [4] Y. S. Amhis *et al.* [HFLAV Collaboration], *Averages of b -hadron, c -hadron, and τ -lepton properties as of 2018*, *Eur. Phys. J. C* **81**, 226 (2021) [arXiv:1909.12524]
- [5] R. Aaij *et al.* [LHCb Collaboration], *Measurement of $|V_{cb}|$ with $B_s^0 \rightarrow D_s^{(*)-} \mu^+ \nu_\mu$ decays*, *Phys. Rev. D* **101**, 072004 (2020) [arXiv:2001.03225]
- [6] R. Aaij *et al.* [LHCb Collaboration], *Measurement of the shape of the $B_s^0 \rightarrow D_s^{*-} \mu^+ \nu_\mu$ differential decay rate*, *JHEP* **12**, 144 (2020) [arXiv:2003.08453]
- [7] J. Harrison *et al.* [HPQCD and (HPQCD Collaboration) \ddagger], *$B \rightarrow D^*$ and $B_s \rightarrow D_s^*$ vector, axial-vector and tensor form factors for the full q^2 range from lattice QCD*, *Phys. Rev. D* **109**, 094515 (2024) [arXiv:2304.03137]
- [8] N. Penalva, J. M. Flynn, E. Hernández and J. Nieves, *Study of new physics effects in $\bar{B}_s \rightarrow D_s^{(*)} \tau^- \bar{\nu}_\tau$ semileptonic decays using lattice QCD form factors and heavy quark effective theory*, *JHEP* **01**, 163 (2024) [arXiv:2304.00250]
- [9] J. Harrison *et al.* [HPQCD Collaboration], *$B_s \rightarrow D_s^*$ form factors for the full q^2 range from lattice QCD*, *Phys. Rev. D* **105**, 094506 (2022) [arXiv:2105.11433]
- [10] J. Harrison *et al.* [HPQCD Collaboration], *Lattice QCD calculation of the $B_{(s)} \rightarrow D_{(s)}^* \ell \nu$ form factors at zero recoil and implications for $|V_{cb}|$* , *Phys. Rev. D* **97**, 054502 (2018) [arXiv:1711.11013]
- [11] E. McLean, C. T. H. Davies, A. T. Lytle and J. Koponen, *Lattice QCD form factor for $B_s \rightarrow D_s^* \ell \nu$ at zero recoil with non-perturbative current renormalisation*, *Phys. Rev. D* **99**, 114512 (2019) [arXiv:1904.02046]
- [12] M. Bordone, N. Gubernari, D. van Dyk and M. Jung, *Heavy-Quark expansion for $\bar{B}_s \rightarrow D_s^{(*)}$ form factors and unitarity bounds beyond the $SU(3)_F$ limit*, *Eur. Phys. J. C* **80**, 347 (2020) [arXiv:1912.09335]
- [13] N. R. Soni, A. Issadykov, A. N. Galaria, Z. Tyulemisov, J. J. Patel and J. N. Pandya, *Form factors and branching fraction calculations for $B_s \rightarrow D_s^{(*)} \ell^+ \nu_\ell$ in view of LHCb observation*, *Eur. Phys. J. Plus* **138**, 163 (2023) [arXiv:2110.12740]
- [14] P. Blasi, P. Colangelo, G. Nardulli and N. Paver, *Phenomenology of B_s decays*, *Phys. Rev. D* **49**, 238-246 (1994) [arXiv:hep-ph/9307290]
- [15] R. N. Faustov and V. O. Galkin, *Weak decays of B_s mesons to D_s mesons in the relativistic quark model*, *Phys.Rev.D* **87**, 034033 (2013) [arXiv:1212.3167]
- [16] Y. Y. Fan, W. F. Wang and Z. J. Xiao, *Study of $\bar{B}_s^0 \rightarrow (D_s^+, D_s^{*+}) l^- \bar{\nu}_l$ decays in the pQCD factorization approach*, *Phys. Rev. D* **89**, 014030 (2014) [arXiv:1311.4965]
- [17] X. Q. Hu, S. P. Jin and Z. J. Xiao, *Semileptonic decays $B/B_s \rightarrow (D^{(*)}, D_s^{(*)}) l \nu_l$ in the pQCD approach with the lattice QCD input*, *Chin. Phys. C* **44**, 053102 (2020) [arXiv:1912.03981]
- [18] G. Li, F. I. Shao and W. Wang, *$B_s \rightarrow D_s(3040)$ form factors and B_s decays into $D_s(3040)$* , *Phys. Rev. D* **82**, 094031 (2010) [arXiv:1008.3696]
- [19] T. Zhou, T. Wang, Y. Jiang, X. Z. Tan, G. Li and G. L. Wang, *Relativistic calculations of $R(D^{(*)})$, $R(D_s^{(*)})$, $R(\eta_c)$ and $R(J/\psi)$* , *Int. J. Mod. Phys. A* **35**, 2050076 (2020) [arXiv:1910.06595]
- [20] P. Ball, V. M. Braun and H. G. Dosch, *Form-factors of semileptonic D decays from QCD sum rules*, *Phys. Rev. D* **44**, 3567-3581 (1991)
- [21] V. L. Chernyak and I. R. Zhitnitsky, *B meson exclusive decays into baryons*, *Nucl. Phys. B* **345**, 137-172 (1990)
- [22] M. A. Shifman, A. I. Vainshtein and V. I. Zakharov, *QCD and Resonance Physics: Applications*, *Nucl. Phys. B* **147**, 448-518 (1979)
- [23] A. Khodjamirian, C. Klein, T. Mannel and Y. M. Wang, *Form Factors and Strong Couplings of Heavy Baryons from QCD Light-Cone Sum Rules*, *JHEP* **09**, 106 (2011) [arXiv:1108.2971]
- [24] Y. L. Yang, H. J. Tian, Y. X. Wang, H. B. Fu, T. Zhong, S. Q. Wang and D. Huang, *Probing $|V_{cs}|$ and lepton flavor universality through $D \rightarrow K_0^*(1430) \ell \nu_\ell$ decays*, *Phys. Rev. D* **110**, 116030 (2024). [arXiv:2409.01512]
- [25] Y. L. Yang, Y. X. Wang, H. B. Fu, T. Zhong and Y. L. Song, *Scrutinizing B^0 -meson flavor changing neutral current decay into scalar $K_0^*(1430)$ meson with $b \rightarrow s \ell^+ \ell^- (\nu \bar{\nu})$ transition*, *Eur. Phys. J. C* **85**, 64 (2025). [arXiv:2410.09363]
- [26] P. Ball and R. Zwicky, *$|V_{ub}|$ and constraints on the leading-twist pion distribution amplitude from $B \rightarrow \pi \ell \nu$* , *Phys. Lett. B* **625**, 225-233 (2005) [arXiv:hep-ph/0507076]
- [27] G. Duplancic, A. Khodjamirian, T. Mannel, B. Melic and N. Offen, *Light-cone sum rules for $B \rightarrow \pi$ form factors revisited*, *JHEP* **04**, 014 (2008) doi:10.1088/1126-6708/2008/04/014 [arXiv:0801.1796]
- [28] A. Khodjamirian, T. Mannel, N. Offen and Y. M. Wang, *$B \rightarrow \pi \ell \nu_l$ Width and $|V_{ub}|$ from QCD Light-Cone Sum Rules*, *Phys. Rev. D* **83**, 094031 (2011) [arXiv:1103.2655]
- [29] X. G. Wu and T. Huang, *Radiative Corrections on the $B \rightarrow P$ Form Factors with Chiral Current in the Light-Cone Sum Rules*, *Phys. Rev. D* **79**, 034013 (2009) [arXiv:0901.2636]
- [30] H. B. Fu, X. G. Wu, W. Cheng and T. Zhong, *ρ -meson longitudinal leading-twist distribution amplitude within QCD background field theory*, *Phys. Rev. D* **94**, 074004 (2016). [arXiv:1607.04937]
- [31] L. Zhang, X. W. Kang, X. H. Guo, L. Y. Dai, T. Luo and C. Wang, *A comprehensive study on the semileptonic decay of heavy flavor mesons*, *JHEP* **02**, 179 (2021). [arXiv:2012.04417].
- [32] M. A. Ivanov, J. G. Körner and C. T. Tran, *Exclusive decays $B \rightarrow \ell^- \bar{\nu}$ and $B \rightarrow D^{(*)} \ell^- \bar{\nu}$ in the covariant quark model*, *Phys. Rev. D* **92**, 114022 (2015). [arXiv:1508.02678].
- [33] M. A. Ivanov, J. G. Körner, J. N. Pandya, P. Santorelli, N. R. Soni and C. T. Tran, *Exclusive semileptonic decays of D and D_s mesons in the covariant confining quark model*, *Front. Phys. (Beijing)* **14**, 64401 (2019). [arXiv:1904.07740].
- [34] P. Ball and V. M. Braun, *Use and misuse of QCD sum rules in heavy to light transitions: The Decay $B \rightarrow \rho e \nu$ Reexamined*, *Phys. Rev. D* **55**, 5561-5576 (1997), [arXiv:hep-ph/9701238].
- [35] S. Wandzura and F. Wilczek, *Sum Rules for Spin Dependent Electroproduction: Test of Relativistic Constituent Quarks*, *Phys. Lett. B* **72**, 195-198 (1977).
- [36] H. B. Fu, L. Zeng, W. Cheng, X. G. Wu and T. Zhong, *Longitudinal leading-twist distribution amplitude of the J/ψ meson within the background field theory*, *Phys. Rev. D* **97**, 074025 (2018) [arXiv:1801.06832]
- [37] D. D. Hu, X. G. Wu, L. Zeng, H. B. Fu and T. Zhong, *Improved light-cone harmonic oscillator model for the ϕ -meson longitudinal leading-twist light-cone distribution amplitude and its effects to $D_s^+ \rightarrow \phi \ell^+ \nu_\ell$* , *Phys. Rev. D* **110** (2024), 056017. [arXiv:2403.10003]
- [38] T. Zhong, Y. H. Dai and H. B. Fu, *ρ -meson longitudinal leading-twist distribution amplitude revisited and the $D \rightarrow \rho$ semileptonic decay**, *Chin. Phys. C* **48** (2024), 063108. [arXiv:2308.14032]
- [39] S. J. Brodsky, J. R. Ellis, J. S. Hagelin and C. T. Sachrajda,

- Baryon Wave Functions and Nucleon Decay*, *Nucl. Phys. B* **238**, 561-581 (1984).
- [40] S. J. Brodsky, C. R. Ji and G. P. Lepage, *Quantum Chromodynamic Predictions for the Deuteron Form-Factor*, *Phys. Rev. Lett.* **51**, 83 (1983).
- [41] T. Huang and Z. Huang, *Quantum Chromodynamics in Background Fields*, *Phys. Rev. D* **39**, 1213-1220 (1989).
- [42] T. Zhong, Y. Zhang, X. G. Wu, H. B. Fu and T. Huang, *The ratio $\mathcal{R}(D)$ and the D -meson distribution amplitude*, *Eur. Phys. J. C* **78**, 937 (2018). [arXiv:1807.03453].
- [43] Y. Zhang, T. Zhong, H. B. Fu, W. Cheng and X. G. Wu, *D_s -meson leading-twist distribution amplitude within the QCD sum rules and its application to the $B_s \rightarrow D_s$ transition form factor*, *Phys. Rev. D* **103**, 114024 (2021). [arXiv:2104.0018].
- [44] Y. Zhang, T. Zhong, X. G. Wu, K. Li, H. B. Fu and T. Huang, *Uncertainties of the $B \rightarrow D$ transition form factor from the D -meson leading-twist distribution amplitude*, *Eur. Phys. J. C* **78**, 76 (2018). [arXiv:1709.02226].
- [45] B. Pullin and R. Zwicky, *Radiative decays of heavy-light mesons and the $f_{H, H^*, H_1}^{(T)}$ decay constants*, *JHEP* **09**, 023 (2021) [arXiv:2106.13617].
- [46] K. C. Yang, W. Y. P. Hwang, E. M. Henley and L. S. Kisslinger, *QCD sum rules and neutron proton mass difference*, *Phys. Rev. D* **47**, 3001-3012 (1993).
- [47] W. Y. P. Hwang and K. C. Yang, *QCD sum rules: Delta - N and Sigma0 - Lambda mass splittings*, *Phys. Rev. D* **49**, 460-465 (1994).
- [48] T. Zhong, Z. H. Zhu, H. B. Fu, X. G. Wu and T. Huang, *Improved light-cone harmonic oscillator model for the pionic leading-twist distribution amplitude*, *Phys. Rev. D* **104**, 016021 (2021) [arXiv:2102.03989].
- [49] T. Zhong, H. B. Fu and X. G. Wu, *Investigating the ratio of CKM matrix elements $|V_{ub}|/|V_{cb}|$ from semileptonic decay $B_s^0 \rightarrow K^- \mu^+ \nu_\mu$ and kaon twist-2 distribution amplitude*, *Phys. Rev. D* **105**, 116020 (2022) [arXiv:2201.10820].
- [50] A. Bharucha, D. M. Straub and R. Zwicky, *$B \rightarrow V \ell^+ \ell^-$ in the Standard Model from light-cone sum rules*, *JHEP* **08**, 098 (2016) [arXiv:1503.05534].
- [51] A. Bharucha, T. Feldmann and M. Wick, *Theoretical and Phenomenological Constraints on Form Factors for Radiative and Semi-Leptonic B-Meson Decays*, *JHEP* **09**, 090 (2010) [arXiv:1004.3249].
- [52] J. N. Pandya, P. Santorelli and N. R. Soni, *Prediction of various observables for $B_s^0 \rightarrow D_s^{(*)-} \ell^+ \nu_\ell$ within covariant confined quark model*, *Eur. Phys. J. ST* **233**, 2075 (2024) [arXiv:2307.14245].
- [53] X. G. Wu and T. Huang, *Heavy and light meson wavefunctions*, *Chin. Sci. Bull.* **59**, 3801 (2014) [arXiv:1312.1455].
- [54] T. Huang, X. N. Wang, X. D. Xiang and S. J. Brodsky, *The Quark Mass and Spin Effects in the Mesonic Structure*, *Phys. Rev. D* **35**, 1013 (1987).